Birefringent properties of diametrically loaded gradient-index lenses

Wei Su and John A. Gilbert

Gradient-index (GRIN) lenses have been widely used as collimators in various fiber-optic sensors and as optical coupling devices in components designed for optical communication systems. However, relatively little attention has been paid to the birefringent properties of GRIN lenses and the potential for using them as photoelastic sensing elements in optical transducers. Analytical and experimental results are described that were obtained for the intensity distribution produced by studying a GRIN lens by using a polariscope. The residual birefringence inherent in an unloaded lens is initially studied. The lens is then assumed to be diametrically loaded and the superposition is studied by the method of ray tracing. When the results obtained from the simulation for a Selfoc, 0.25-pitch lens are compared with experimental data, an excellent agreement is obtained. Intensity increases monotonically with load, confirming that the lens would be a good choice for the sensing element of an optical transducer designed as part of a strain or acceleration measurement system. The numerical simulation is then used to study the influence of residual stress on sensitivity.

Key words: Gradient-index lenses, polarization analysis and measurement, ray tracing.

1. Introduction

A gradient-index (GRIN) lens is an optical rod in which the refractive index changes radially but remains constant over the length; in most cases, the index profile can be expressed in the form of a parabolic function. The small size of the lens permits compact optical systems to be constructed; flexibility is increased, often permitting the associated optical systems to be designed with fewer optical components. GRIN lenses have been widely used as collimators in various fiber-optic sensors and as optical coupling devices in components designed for optical communication systems, such as laser diodes, fiber-optic transmitters, and fiber-optic connectors.[1]

Even though GRIN lenses have been widely used as sensing elements in displacement transducers, relatively little attention has been paid to their photoelastic properties and potential use as photoelastic sensing elements. This is due mainly to the relatively low stress optic coefficient of the borosilicate glass used to make the lens, coupled with a lack of knowledge regarding the inherent birefringent properties.

We recently introduced a photoelastic fiber-optic strain gauge that relies on an optical transducer consisting of a unidirectionally loaded photoelastic cube sandwiched between two linear polarizing elements.[2] Light was introduced and collected from the sensing element by using multimode optical fibers. Results showed that the system could be used to make both static and dynamic strain measurements. The main requirements for the sensing element are that it has an adequate stress optic coefficient and is compatible with the fiber coupling elements. The loading and geometry must also be optimized to produce the desired intensity modulation. This paper shows that a gradient index lens meets all of these requirements, making the lens an ideal candidate for use in a photoelastic fiber-optic sensor.

Photoelastically induced intensity modulation in GRIN lenses was first reported by Abdulhalim and Pannel in 1993.[3] In their experiment, a GRIN lens was diametrically loaded between two aluminum plates by using a piezoelectric transducer. A He–Ne laser having a wavelength of 633 nm was launched into a single-mode fiber, which served as the light source for a polariscope constructed by using two crossed linear polarizers and one quarter-wave plate. Stress-induced birefringence was estimated by recording the changes in light intensity.

W. Su is at MRL, Inc., 5653 Stoneridge Drive, Suite 102, Pleasanton, California 94588. J. A. Gilbert is with the Department of Mechanical and Aerospace Engineering, University of Alabama in Huntsville, Huntsville, Alabama 35899.

Received 1 November 1995; revised manuscript received 18 March 1996.

0003-6935/96/244772-10$10.00/0

Although Abdulhalim and Pannel were the first to illustrate the potential of using a GRIN lens as a robust and compact photoelastic sensor, they neglected to include the shear stress component in the stress distribution given for the diametrically loaded lens, incorrectly assumed that the longitudinal stress component in the constitutive equations vanishes for the case of plane strain, and did not take the stress concentration at the loading point into account when computing the overall stress distribution in the lens.

In the following sections we describe analytical and experimental results obtained for the intensity distribution produced by studying a GRIN lens with a polariscope. The residual birefringence inherent in an unloaded lens is initially studied. The lens is then assumed to be diametrically loaded and studied by the method of ray tracing. When the results obtained from the simulation for a Selfoc, 0.25-pitch lens are compared with experimental data, excellent agreement is obtained. Intensity increases monotonically with load, confirming that the lens would be a good choice for the sensing element of an optical transducer designed as part of a strain or acceleration measurement system. The numerical simulation is then used to study the influence of residual stress on sensitivity.

2. Residual Birefringence

Ion exchange is the only known method that has been commercially developed for the production of GRIN lenses.[1] During the fabrication of Selfoc microlenses, for example, one can make a preform by immersing a cylindrical borosilicate glass rod containing Tl^+ and Na^+ ions into a high-temperature molten KNO_3 salt bath.[4] Ion diffusion occurs within the glass, leading to the partial substitution of Tl^+ and Na^+ ions by K^+ ions from the salt bath. As the ion exchange process progresses, a nearly parabolic refractive-index distribution, corresponding to the Tl^+ ion concentration, is formed within the rod. After a specified time, typically 10–99 h, the preform is removed from the bath and cut into relatively short segments to produce GRIN lenses of a desired pitch. The ends of each lens are then polished flat.

It is well known that stresses introduced during an ion-exchange process contribute to birefringence in gradient index glass.[5–8] These stresses are caused by either a mole volume change caused by the mismatch in ionic size of exchanging ion pairs, or by the change in thermal properties caused by a variation in glass composition. During the fabrication of a Selfoc lens, the exchange temperature is between the transformation temperature, T_g, and the softening temperature of the glass[4]; consequently, the stresses introduced by the change in mole volume are compensated by the viscous flow that occurs above T_g. Therefore, in the case of a GRIN lens, stresses are introduced because of the variation in the coefficient of linear thermal expansion across the GRIN region. As the lens cools from the transformation temperature to room temperature, residual stresses are introduced. The stress state changes with the working temperature and is modified when external loads are applied to the lens.

In a GRIN lens, the composition of glass can be specified as a function of position[4]; the thermal expansion coefficient is given by

$$\alpha_L(r, \theta, z) = \sum_i \alpha_i p_i(r, \theta, z), \tag{1}$$

where α_i is the partial linear expansion factor for the ith component; the mole fractions, $p_i(r, \theta, z)$, are functions of position.

The thermal expansion coefficient, $\alpha_L(u, v)$, can also be expressed as a departure from that of the base glass, $\alpha_L(0, 0)$, as

$$\alpha_L(u, v) = \alpha_L(0, 0) + [\alpha_K + (\alpha_{Tl} - \alpha_K)u]p_{Tl^+} + [\alpha_K + (\alpha_{Na} - \alpha_K)v]p_{Na^+}, \tag{2}$$

where u and v are exchange parameters for Tl^+ and Na^+, respectively; α_{Tl} and α_{Na} are the partial expansion factors of the exchange oxides; α_K is the partial expansion factor of the diffusing oxide; and p_{Tl^+} and p_{Na^+} are the mole fractions of the two exchange ion components corresponding to Tl^+ and Na^+ before exchange, respectively.

A number of different partial expansion factors are documented in the literature,[5,8,9] and some of these have been applied with Eq. (2) to determine the thermal expansion coefficients for commercially available glasses at an elevated temperature. These analytical predictions typically agree to within a few percent of experimentally measured values.

According to the manufacturer, the distribution of the Tl^+, Na^+, and K^+ ions in Selfoc lenses is basically parabolic.[10] Therefore, the two exchange parameters can be written as

$$u = v = 1 - \chi\left(\frac{r}{R}\right)^2, \tag{3}$$

where χ is a constant depending on the amount of exchange ions remaining at the edge of the GRIN lens; χ typically has a value close to 1.0.

By combining Eqs. (2) and (3), we see that the distribution of thermal expansion coefficients is

$$\alpha_L(r) = \alpha_0 + \left[1 - \chi\left(\frac{r}{R}\right)^2\right][(\alpha_{Tl} - \alpha_K)p_{Tl^+} + (\alpha_{Na} - \alpha_K)p_{Na^+}], \tag{4}$$

where

$$\alpha_0 = \alpha_{LO} + \alpha_K(p_{Tl^+} + p_{Na^+}). \tag{5}$$

In Eq. (5), α_{LO} is thermal expansion coefficient of the original glass.

If the glass rod were removed from the very hot salt bath (~540 °C) and rapidly cooled to room temperature, large aberrations would occur. These aberrations would result in poor optical quality. Consequently, the manufacturer reports that steps are taken to decrease the temperature slowly and

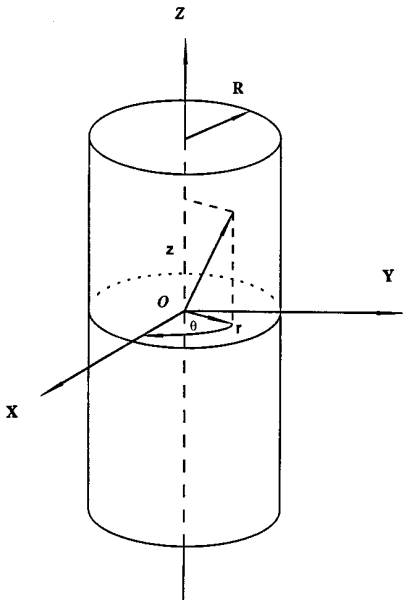

Fig. 1. Coordinate system used for the analysis of thermal stresses.

gradually.[11] Therefore, it is reasonable to assume that the temperature distribution within the rod is uniform as the glass goes through its transformation temperature.

The thermal stress distribution in a long circular cylinder (corresponding to the GRIN lens preform) can be analyzed by the theory of elasticity.[12] Referring to Fig. 1, we find that the temperature is assumed to be equal to room temperature, T, and independent of the coordinates. Under these conditions, a state of plane strain is assumed in which the axial displacement, w, is zero throughout. For the radially symmetric case referred to the axis system shown, all three of the shear stresses and shear strains are zero.

The principal stress difference, R_T, which will be observed in a circular polariscope, is[13]

$$R_T = \sigma_r - \sigma_\theta = \frac{(T - T_g)E}{1 - v}\left(\alpha_L - \frac{2}{r^2}\int_0^r \alpha_L r \, dr\right), \quad (6)$$

where E is the elastic modulus and v is the Poisson ratio. The thermal expansion coefficient, α_L, is a function of the radius.

Substituting Eq. (4) into Eq. (6), we find that

$$R_T = \alpha_G \frac{\chi(T - T_g)E}{2(1 - v)}\left(\frac{r}{R}\right)^2, \quad (7)$$

where

$$\alpha_G = (\alpha_{Tl} - \alpha_K)p_{Tl^+} + (\alpha_{Na} - \alpha_K)p_{Na^+}. \quad (8)$$

For a given GRIN lens, α_G is constant. The principal stress difference given by Eq. (7) is proportional to the residual birefringence. It is clear from this equation that the principal stress difference is radially symmetric and a parabolic function of the radius; it is zero at the center of the lens, attains a maximum value around the circumference, and decreases with increasing room temperature. The value of R_T can be calculated by knowing the temperature and the mechanical and thermal properties of the lens.

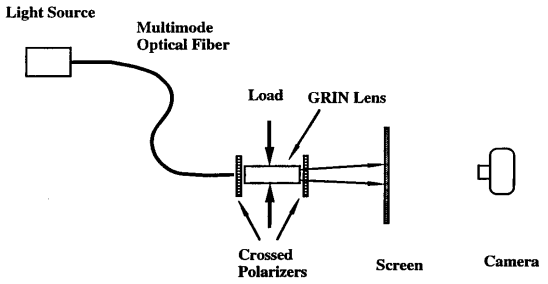

Fig. 2. Experimental setup used to study the GRIN lens with a white-light source and a dark-field plane polariscope.

It is important to point out that the results from Eq. (7) are accurate only if the material properties (i.e., E, v, and α_i) remain constant between room temperature and the transformation temperature. From a practical standpoint, these properties are affected by temperature, especially when the glass is close to the transformation temperature. The violation of this assumption causes an error when the magnitude of the birefringence is calculated; however, the distribution remains the same.

For the above arguments to be verified, a 1-mm diameter, 0.25-pitch, Selfoc, SLW-1.0, GRIN lens was placed in the setup shown in Fig. 2. As shown in the figure, the lens was illuminated by using a point source of white light emitted from a multimode fiber. The end of the fiber was positioned as close as possible to the GRIN lens so that the light emerging from the lens was nearly collimated. The output from the dark-field plane polariscope was observed on a diffusing glass screen positioned immediately behind the analyzer. Figure 3 shows the dark cross observed on the screen when no loads were applied to the lens. The cross formed parallel to the direction of the po-

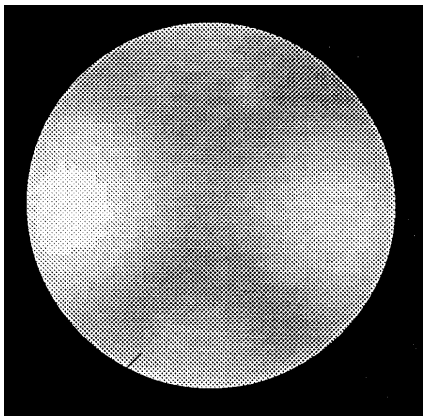

Fig. 3. Combined isochromatic and isoclinic patterns obtained from the setup shown in Fig. 2 for an unloaded GRIN lens.

larizers and rotated with them as they were rotated. This behavior, characteristic of an isoclinic, defines the principal directions of birefringence as radial and tangential, confirming that the induced birefringence is radially symmetric.

The isoclinic pattern was eliminated by inserting one quarter-wave plate between the polarizer and the lens and another between the lens and the analyzer. The fast axis of one plate was aligned with the slow axis of the other; both plates were inserted at 45° with respect to the axes of the polarizers to form a dark-field circular polariscope. In the unloaded state, a circular black spot was observed at center of the GRIN lens. This isochromatic pattern indicates that the birefringence is zero at the center of the lens, whereas the symmetry of the pattern confirms that the birefringence is radially symmetric. The increase in intensity with the distance measured from the center to the outside of the lens signifies a corresponding increase in birefringence.

To our knowledge, the phenomena described above have not been previously reported in the literature. Apparently, the speckles produced by the laser source in Abdulhalim's experiment precluded his group from making these observations. It should be noted that patterns similar to those obtained from the GRIN lens have been observed when traditional optical lenses are studied, even when the birefringence has been carefully removed by the process of annealing. This can be attributed to the well-known fact that the transmission of light at the interface between two different media is determined by the refractive indices of the media and the polarization state of the impinging light. Even though the geometric factors and material properties of the GRIN lens produce effects similar to those observed in a traditional lens, they are secondary when compared with the residual birefringence introduced during fabrication. An additional test was conducted to verify this assumption.

In this test, the temperature of the environment surrounding the 0.25-pitch GRIN lens was elevated to 100 °C and the lens was allowed to achieve thermal equilibrium. When the lens was studied with a circular polariscope, it was observed that the size of the central black spot increased significantly over that observed at room temperature. Because the changes in geometry and the index gradient are extremely small, the changes in the spot size can be attributed only to the change in birefringence introduced when the lens was produced.

3. Stress-Induced Birefringence

When diametrical compressive loads are applied uniformly along the length of the lens, a state of plane strain is assumed. The stress-induced birefringence may be calculated from the stress distribution in the GRIN lens. Assuming that the loading conditions are the same for all cross sections, we see that the stress distribution is identical for all thin disks numerically cut from the lens along the Z axis. Figure 4 shows a disk subjected to concentrated diametrical line loads P across its thickness. In this case, the

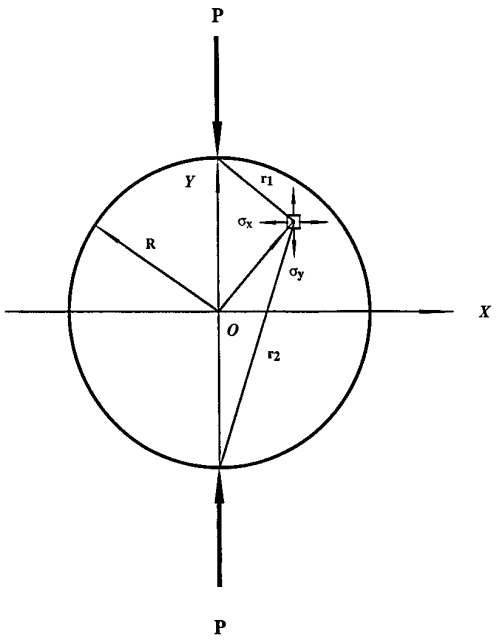

Fig. 4. Schematic diagram, showing a disk subjected to concentrated diametrical line loads and the associated rectangular stress components.

stresses are given by[14]

$$\sigma_x = -\frac{2P}{\pi t}\left[\frac{(R-y)x^2}{r_1^4} + \frac{(R+y)x^2}{r_2^4} - \frac{1}{2R}\right], \quad (9)$$

$$\sigma_y = -\frac{2P}{\pi t}\left[\frac{(R-y)^3}{r_1^4} + \frac{(R+y)^3}{r_2^4} - \frac{1}{2R}\right], \quad (10)$$

$$\tau_{xy} = \frac{2P}{\pi t}\left[\frac{(R-y)^2x}{r_1^4} - \frac{(R+y)^2x}{r_2^4}\right], \quad (11)$$

where

$$r_1^2 = x^2 + (R-y)^2, \qquad r_2^2 = x^2 + (R+y)^2. \quad (12)$$

In Eqs. (9)–(12), σ_x and σ_y are normal stresses, τ_{xy} is the shear stress, and R and t are the radius and thickness of the disk, respectively. The remaining two shear stresses, τ_{xz} and τ_{yz}, are zero, whereas the longitudinal normal stress σ_z can be expressed in terms of σ_x and σ_y by using Hooke's law. For plane strain, $\varepsilon_z = 0$, and

$$\sigma_z = v(\sigma_x + \sigma_y), \quad (13)$$

where v is Poisson's ratio.

When a light ray travels nearly parallel to the direction of one principal stress, the contribution of that principal stress to the temporary birefringence has a negligible effect on the state of polarization (SOP).[15] Because the light rays propagating within a GRIN lens remain predominately in the paraxial region (nearly parallel to the Z axis), the contribution of σ_z to the birefringence can be neglected and only the in-plane stress components need be considered.

In the X–Y plane, the principal stresses are ori-

ented at an angle, θ, measured with respect to the X axis, where

$$\theta = \frac{1}{2}\tan^{-1}\left(\frac{2\tau_{xy}}{\sigma_x - \sigma_y}\right). \tag{14}$$

The difference between the principal stresses σ_d is

$$\sigma_d = [(\sigma_x - \sigma_y)^2 + 4{\tau_{xy}}^2]^{1/2}. \tag{15}$$

Because the residual stress is radially symmetric, the angle of orientation corresponding to the superimposed residual and stress-induced birefringence is found simply by substituting Eqs. (9)–(12) into Eq. (14). The result is

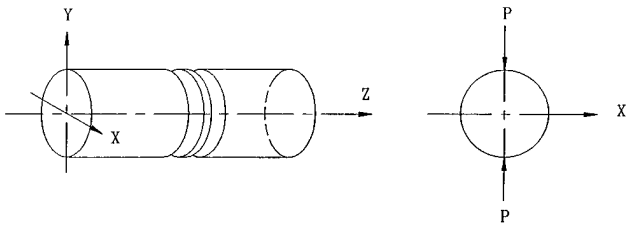

Fig. 5. Coordinate system used for the analysis of the GRIN lens.

$$\tan 2\theta = 2\,\frac{\dfrac{(R-y)^2x}{(R-y)^2+x^2} - \dfrac{(R+y)^2x}{(R+y)^2+x^2} + \dfrac{\pi t_t}{2P}\sigma_T\dfrac{xy}{R^2}}{(R-y)\dfrac{(R-y)^2-x^2}{(R-y)^2+x^2} + (R+y)\dfrac{(R+y)^2-x^2}{(R+y)^2+x^2} + \dfrac{\pi t_t}{2P}\sigma_T\dfrac{y^2-x^2}{R^2}}, \tag{16}$$

where the quantity

$$\sigma_T = \alpha_G\frac{\chi E(T - T_g)}{2(1-v)} \tag{17}$$

is the thermally induced residual stress at the circumference of the GRIN lens.

One can compute the difference between the principal stresses, in contrast, first by applying a coordinate transformation to Eqs. (7) and (8) and then superimposing the result with the stress difference found by substituting Eqs. (9)–(12) into Eq. (15). The result is

$$\begin{aligned}{\sigma_d}^2 = \frac{4P^2}{\pi^2{t_t}^2}\Bigg\{&\Bigg[(R-y)\frac{(R-y)^2-x^2}{(R-y)^2+x^2} \\ &+ (R+y)\frac{(R+y)^2-x^2}{(R+y)^2+x^2} + \frac{\pi t_t}{2P}\sigma_T\frac{xy}{R^2}\Bigg]^2 \\ &+ 4\Bigg[\frac{(R-y)^2x}{(R-y)^2+x^2} - \frac{(R+y)^2x}{(R+y)^2+x^2} \\ &+ \frac{\pi t_t}{2P}\sigma_T\frac{xy}{R^2}\Bigg]^2\Bigg\}.\end{aligned} \tag{18}$$

4. Tracing the Polarization State

Before the diametrically loaded GRIN lens can be modeled, it is necessary to develop an algorithm that permits the state of polarization to be calculated throughout the lens. The mechanics of polarization ray tracing was recently summarized by Chipman.[16] The basic method has two steps: first to determine the coordinates of the ray intercepts at each interface and the propagation vector by means of geometrical ray tracing in the optical system, second to calculate the evolution of the propagation vector along a ray path by using the data from the previous step and by applying the polarization properties of the medium.

The ray equation for an inhomogeneous medium is

$$\frac{\mathrm{d}}{\mathrm{d}s}\left[n(\mathbf{r})\frac{\mathrm{d}\mathbf{r}}{\mathrm{d}s}\right] = \nabla n(\mathbf{r}), \tag{19}$$

where $n(\mathbf{r})$ is the index of refraction and $\mathbf{r}$ is the position vector of a point on the ray.

Several numerical methods have been developed to trace rays traveling through an inhomogeneous medium. The numerical algorithm developed by Sharma,[17] for example, transforms the ray equation into a convenient form for numerical integration. The approach defines a new variable and solves the resulting equation by using a standard numerical technique such as the Runge–Kutta method. Because of its simplicity and accuracy, Sharma's algorithm is adopted and modified to study the GRIN lens.

The rectangular coordinate system shown in Fig. 5 was defined in an effort to solve Eq. (19). The optical axis of the GRIN lens is assumed to be positioned along the Z axis. A point source is located on the Z axis at a distance z_o, from the front surface of the lens. After the light emitted from the source is refracted by the lens, it intersects the Z axis in the image plane located at a distance z_i, measured from the rear surface of the lens. The location of a point on the light ray is given by position vector $\mathbf{r}(x, y, z)$.

The expression describing the refractive-index distribution in the GRIN lenses is given by the manufacturer as[18]

$$n(r) = n_0\left(1 - \frac{A}{2}r^2\right), \tag{20}$$

where n_0 is the refractive index at the center of the lens, A is the index gradient constant, and $r(x, y)$ is

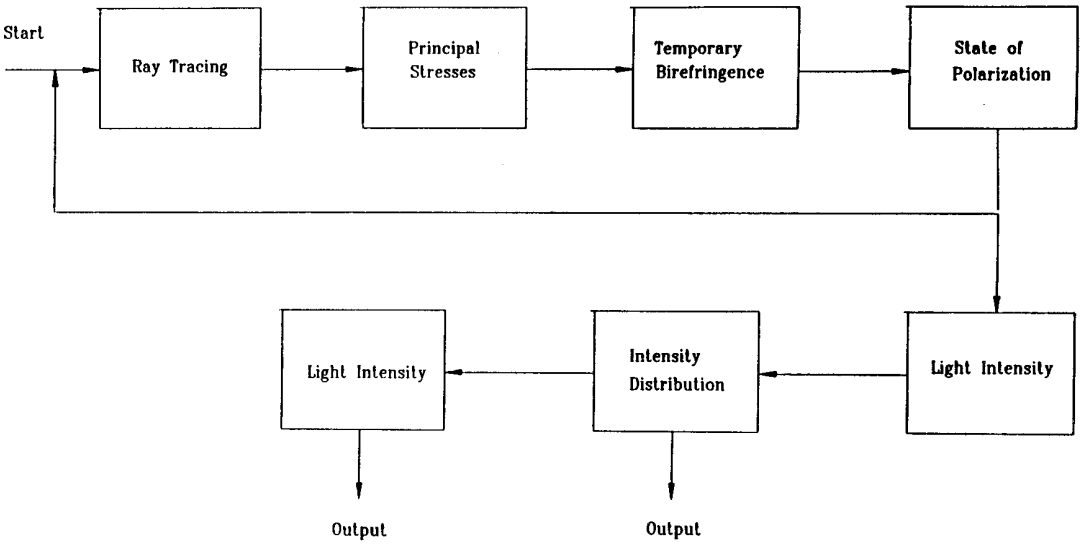

Fig. 6. Flow diagram for ray tracing.

the distance from the optical axis. The refractive index is constant along the Z axis.

The relative optical linear retardation is given by

$$R_r = C\sigma_d \frac{tn(r)}{\Gamma_z}, \tag{21}$$

where C is the relative stress optic coefficient and Γ_z is the direction cosine of the light ray with respect to the Z axis; σ_d is obtained from Eq. (18).

The stress optic coefficient of the GRIN lens is relatively low, and calculations that use Eq. (21) show that, when the lens is subjected to a load equal to 20 N, the temporary birefringence is of the order of 1×10^{-4}. This value is extremely small compared with the change in index of refraction (0.07) across the lens, and neglecting it in the ray-tracing algorithm will not significantly affect the path. Consequently, when the ray-tracing algorithm is formulated for the GRIN lens, the medium is assumed to be optically isotropic.

From a conceptual standpoint, the calculation procedure starts by numerically slicing the GRIN lens into a number N of thin disks, each having a thickness equal to $(n\,\Delta\,\xi)$. This is illustrated in Fig. 5. It should be noted, however, that in the formulation of Eq. (21), the path length of the light ray propagating through the disk is used, as opposed to the thickness of the disk. The optical and mechanical properties are assumed to be constant over the thickness of each disk. Therefore, ray tracing is analogous to characterizing ray propagation through N identical optical elements.

As discussed by Chipman,[16] the Jones vector provides a description of the polarization in the plane normal to the direction of propagation of a ray; relations are defined with respect to two orthogonal (local) coordinate axes. In this paper, the state of polarization is represented by a polarization vector defined with respect to a global Cartesian axes system. The angle between the propagation vector and the Z axis is small because the paraxial ray is studied; consequently, the Jones vector can be defined by two orthogonal global coordinates, X and Y, without introducing large errors.

One can determine the state of polarization of the light passing through the GRIN lens by assuming that linearly polarized light rays emerge from a point source. Each ray is initially traced through the lens; Fig. 6 shows the flow chart for the procedure. The position and propagation vector of the ray is computed at each numerical interface. With the knowledge of the position and the stress distribution in a given element, one can calculate the temporary birefringence. The Jones matrix is constructed and applied to determine the SOP of the light transmitted through the element. The SOP from the first element is used as the input for the second. The process is continued over the length of the GRIN lens to predict the final SOP.

5. Numerical Simulation of Light Intensity

The intensity modulation caused by mechanically and thermally loading a GRIN lens in a dark-field plane polariscope was numerically simulated. When applying the numerical model, one can assume the input light to be of intensity I_0 and linearly polarized at an angle, α_p, with respect to the x axis. After the input light passes through the GRIN lens, the two normal components of polarization are combined at the analyzer and the intensity for a given ray is calculated.

As suggested by Chipman,[16] a ray can be considered to represent a small portion of the wave front at the front surface of the lens that subtends a fixed solid angle measured from the object point. Consequently, the amplitude of the components in a Jones vector represents an electric field times an area on the front surface of the GRIN lens. By averaging the

Table 1. Parameters for the Numerical Simulation of a GRIN Lens

Parameters	Values
N_0	1.5986
R	0.5 mm
z_e	2.61 mm
A	0.3612 mm^{-1}
C	2.74×10^{-6} mm^2/N
λ	0.82 μm
$\Delta\xi$	0.01 mm
z_o	1.5 mm
z_i	2.0 mm
σ_T	20 N/mm

light intensities for all rays across the image, one obtains a relative measure of the overall intensity.

Rigorously, the corresponding electric fields should be added because the results may show interference patterns. However, because of the existence of aberrations in the GRIN lens, the light rays from a point source are not focused to a single point in the image plane. When using an incoherent light source and by collecting the light from the GRIN lens with a multimode optical fiber, we find that the effect of any interference is small. Therefore, the light rays may be added by intensity instead of by electric field.

The procedure outlined above was applied to analyze a 1-mm-diameter, 0.25-pitch, Selfoc, SLW-1.0, GRIN lens. The geometric and optical parameters required for the computer simulation are listed in Table 1.[18]

Because the fiber was positioned at a distance of 1.5 mm from the front surface of the lens, which had an effective diameter of 0.6 mm, it was assumed that all the light rays entering the lens were of equal intensity. The analysis was performed using a 40×40 rectangular grid corresponding to the intersection of the illuminating rays with a plane positioned at the front face of the GRIN lens. Contour maps of the intensity distribution in the paraxial focal plane, where the size of the image is minimum, were plotted. The fringe contours on each plot represent different values of the light intensity; the relative intensity of each contour is included on the plots.

The intensity distribution for the case in which the polarizers are oriented at 45° with respect to the vertical and no external loads are applied is shown in Fig. 7; the intensity distribution is similar to that obtained in the experiments performed with a plane polariscope and shown in Fig. 3. The match between the patterns confirms that the hypothesis and the associated analysis for the residual stresses were correct. The contrast of the pattern depends on the level of the thermally induced stress in the GRIN lens.

Figure 8, in contrast, shows typical intensity distributions obtained as the diametrical load was progressively increased from 0 to 20 N. In general, as the load increases, the highly stressed areas under the loading points become bright. The stress distribution also changes and the dark cross, originally

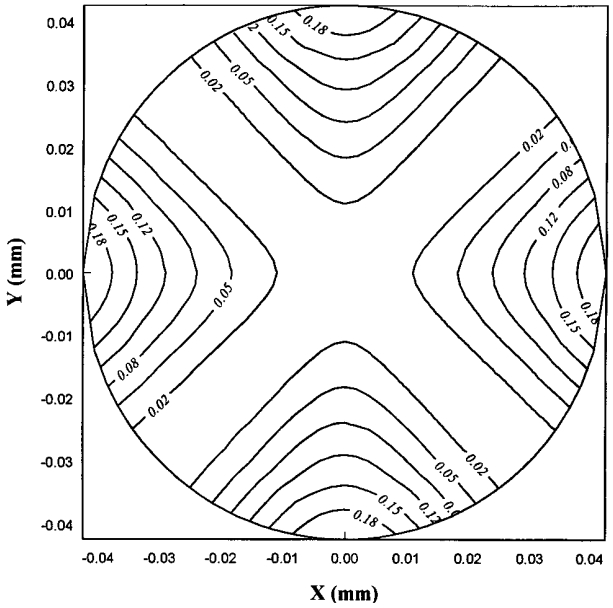

Fig. 7. Intensity distribution at the image plane of an unloaded GRIN lens.

observed along the directions of the polarizers at no load, distorts. The intensity modulation caused by the change in stress distribution (isoclinics) and stress level (isochromatics) causes the overall intensity to increase monotonically with load. Figure 9 shows a plot of the light intensity versus the diametrical load as computed from this simulation.

6. Experimental Verification and Comparison

For these analytical results to be verified, a 1-mm diameter, 0.25-pitch, Selfoc, SLW-1.0, GRIN lens was placed in the setup shown in Fig. 2. The lens was compressed by applying loads along the diameter with a pneumatic actuator. As loads were applied, the cross produced by the residual stress gradually disappeared; two bright spots were observed at the top and bottom of the pattern, close to the loading points. The changes in the isoclinic pattern showed that a redistribution of stress took place within the lens; the patterns display characteristics similar to those observed in Fig. 8.

After these observations, the screen was replaced by a second multimode optical fiber, which collected the light from the GRIN lens and guided it to a photodetector. The position of the optical fibers was adjusted to maximize the coupling efficiency. Figure 10 shows the intensity of the light recorded from the dark-field plane polariscope as loads were applied. The increase in light intensity is nearly linear; the nonlinear region at low load was partially attributed to poor initial contact between the lens and the actuator.

The experimental and analytical results are best compared by introducing the following definition[13] for

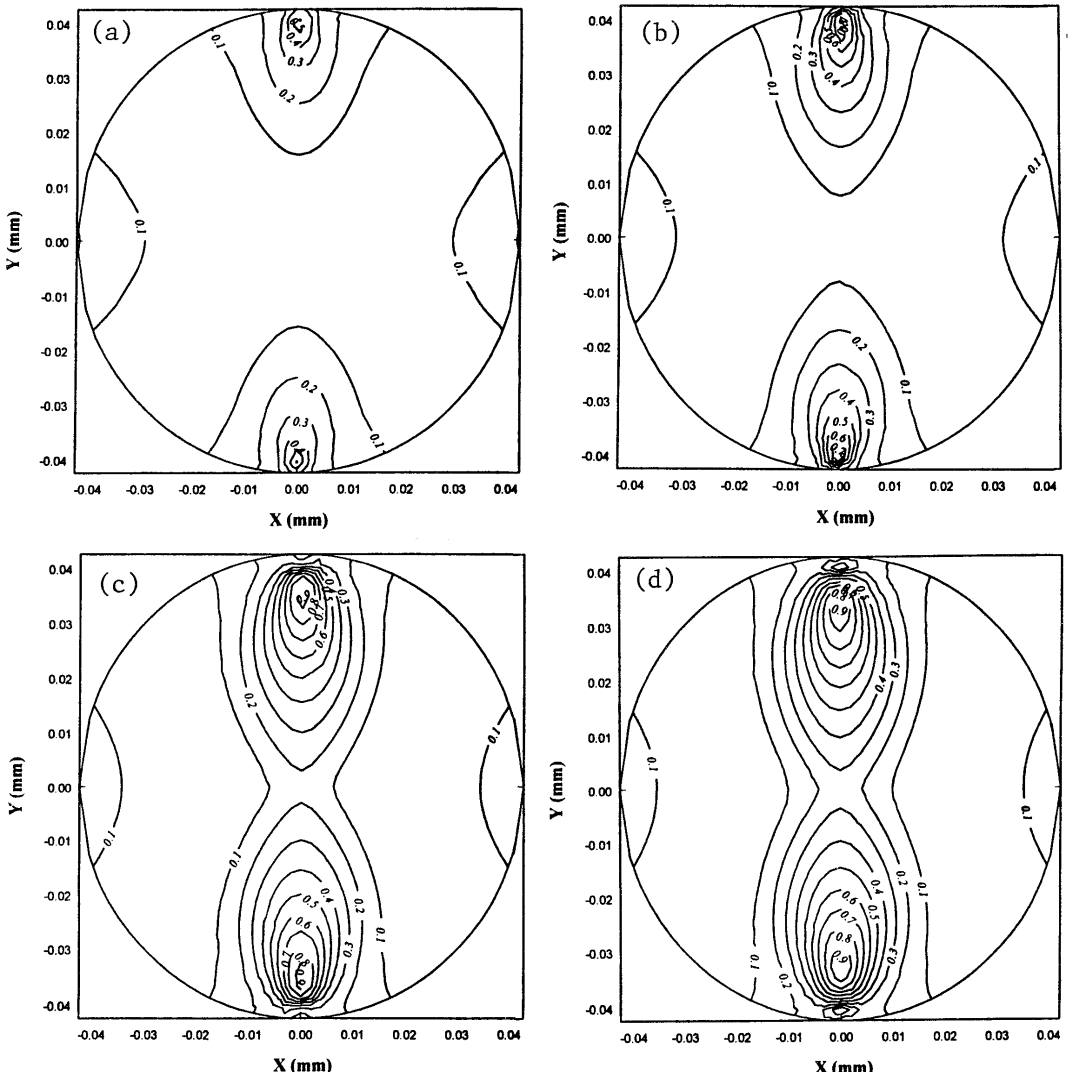

Fig. 8. Intensity distribution at the image plane of a GRIN lens for (a) $P = 4$ N, (b) $P = 8$ N, (c) $P = 16$ N, (d) $P = 20$ N.

the sensitivity S_l:

$$S_l = \frac{\Delta I / I_h}{\Delta P}, \tag{22}$$

where ΔI is the change in light intensity that occurs when the diametrical load is modulated through ΔP. Because I_h is the average value of the light intensities observed when minimum and maximum loads are applied, computed with

$$I_h = \frac{1}{2}\,(I|_{P=P_{\min}} + I|_{P=P_{\max}}), \tag{23}$$

the sensitivity is expressed in terms of $(\text{newtons})^{-1}$. In practice, the light intensity I_h is an important parameter that can be used to define the sensitivity required of the photodetector that receives the signal. The numerical and experimental values computed from Eq. (21) are 0.0742 and 0.0756 N^{-1}, respectively; the error is less than 2%.

7. Influence of Residual Stress on Sensitivity

The sensitivity of the transducer is affected by the thermally induced residual stress level in the GRIN lens. Unfortunately, the latter cannot be quantified at present, because there is insufficient data with which to calculate the value of an equivalent thermal expansion coefficient. However, the maximum stress level measured in other studies,[7,8] in which the change in mole volume was predominant, has been reported as high as 1000 N/mm^2. Because this is not the case for the GRIN lens, the stress level was assumed to be much smaller.

A study was performed by assuming that the maximum value of the thermally induced residual stress, prescribed along the circumference of the lens, varied between 0 and 60 N/mm^2. Plots of the intensity versus load are shown in Fig. 11. In general, the intensity increases with increasing residual stress. When the residual stress is zero, the response of the transducer is the most nonlinear. The response is nearly linear in the range between 40 and 60 N/mm^2;

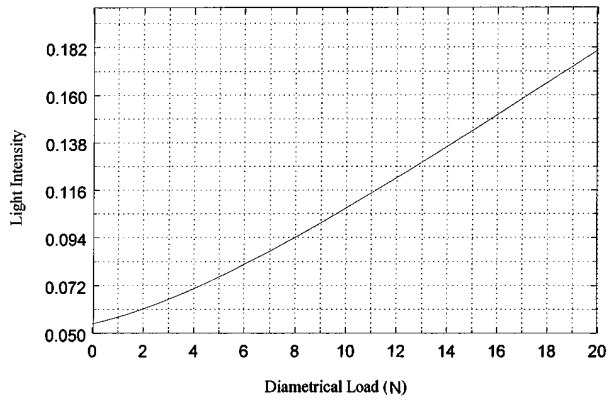

Fig. 9. Light intensity versus the diametrical load as computed from the numerical simulation.

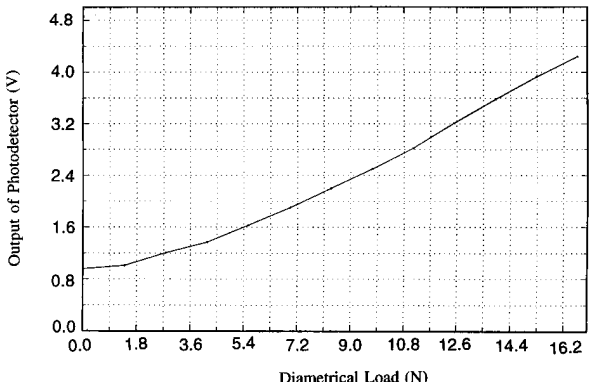

Fig. 10. Plot of the intensity obtained from the plane polariscope as diametrical loads were applied to the GRIN lens.

above this value the response again becomes nonlinear. It is also important to note that the sensitivity decreases with increasing residual stress. As the maximum residual stress increases from 20 to 60 N/mm^2, the sensitivity is reduced by 7.5 times.

From this analysis, it is evident that the ideal transducer would be constructed by using a GRIN lens that had a residual stress equal to approximately 40 N/mm^2. This would result in the highest sensitivity and the largest range over which the response was linear. As discussed above, the level of residual stress is mainly determined by the mechanical properties of the exchanging ions; this process may be difficult to control.

Equation (7) shows that the level of residual stress is directly proportional to the ambient temperature. Based on the use of the arguments outlined above, an increase in the temperature will reduce the level of the residual stress, leading to a more nonlinear response and a decrease in sensitivity. These effects could be minimized in future designs by reducing the equivalent thermal expansion coefficient of the lens.

8. Error Analysis

The experimental results deviate slightly from those obtained by using the numerical algorithm. Quantitatively, an error arises from the assumption that light is launched from a point source along the optical axis. Strictly speaking, this is not true because the effective diameter of the GRIN lens is 0.6 mm and light is launched from a distance of 1.5 mm by using a fiber with a core diameter equal to 0.2 mm. To eliminate the associated error, one would have to

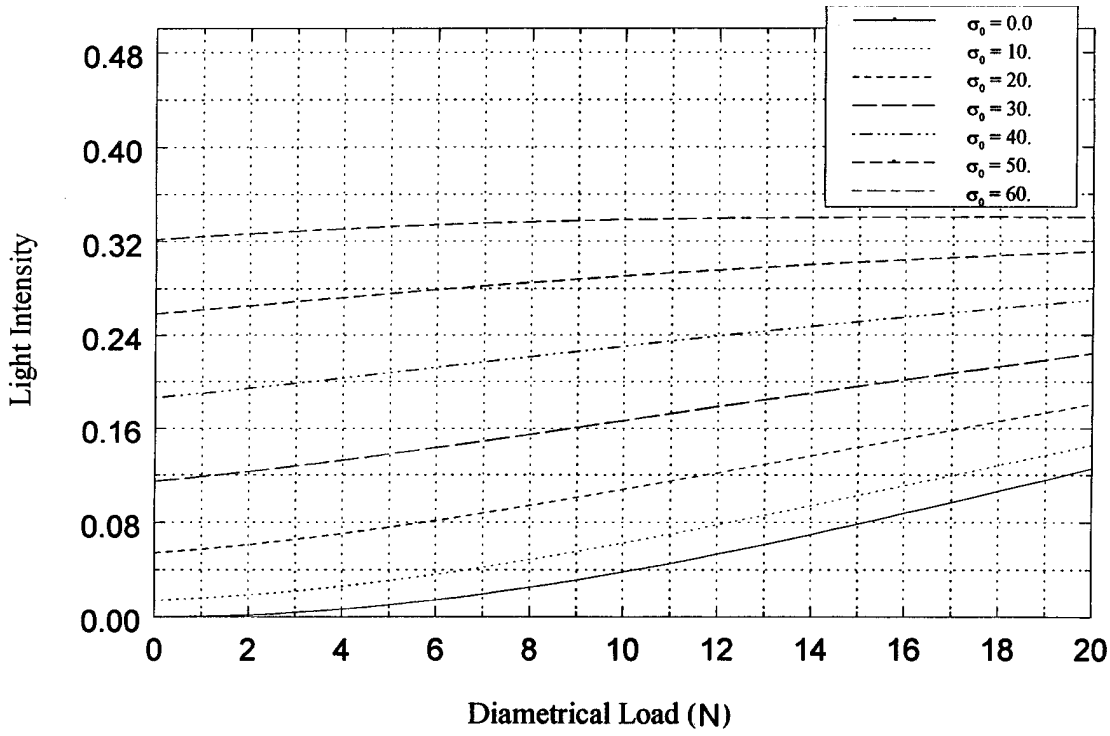

Fig. 11. Intensity versus diametrical load at various levels of residual stress.

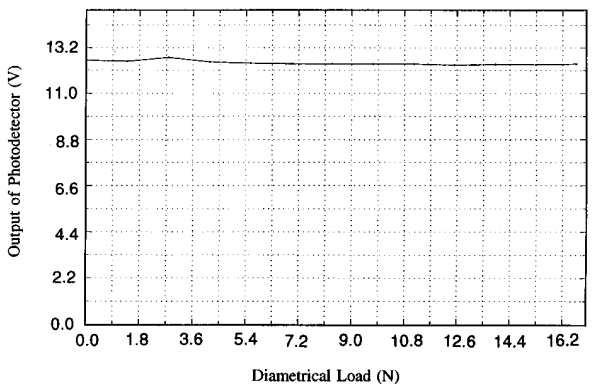

Fig. 12. Intensity versus diametrical load without the use of a polariscope.

consider the light rays coming from a distributed light source. However, in this case, the on-axis and off-axis points composing the distributed source would produce similar light intensity distributions in the image plane, and the trends we observed by considering a single on-axis point source would most likely be analogous.

When the source is different from a point, other intensity modulations may occur because of the aberrations (spherical aberration, coma, astigmatism, and distortion) caused by off-axis rays.[19] In this case, the stress-induced temporary birefringence could modulate the aberrations, thereby changing the spatial intensity distribution but not the average intensity of the pattern. These effects could be important to quantify, especially when the receiving fiber has a relatively small diameter compared with the spot size, as in the case reported by Abdulhalim and Pannel.[3] Because the light received by the fiber would depend on its relative position with respect to the spot, the change in aberration would strongly influence the detected signal.

However, the effect described above can be minimized by using a relatively large (of the order of 200-μm) diameter multimode fiber to sample the image plane. As a way to verify that such a fiber was sufficient, one of the polarizers in the setup shown in Fig. 2 was removed. Figure 12 shows a plot of the light intensity versus the loads applied to the GRIN lens. The intensity is nearly a constant, indicating that changes in aberration within the lens do not significantly affect the output from the photoelastic fiber-optic transducer.

9. Conclusions

In conclusion, the potential of using a GRIN lens as a coupling–sensing element in a fiber-optic transducer has been demonstrated experimentally. The optical response to load has been characterized by taking into account the residual birefringence produced in the lens during fabrication. The results from numerical simulations agree well with the experimental data, and numerical algorithms were applied to study the effect of residual stress on sensitivity. When a plane polariscope configuration is used, the existence of the residual stress in the GRIN lens actually reduces the nonlinear response of the transducer.

The authors acknowledge that many productive discussions regarding the subject matter contained herein were held with Don Gregory, Larry Pezzaniti, and Shih-Yau Lu of the Department of Physics at the University of Alabama in Huntsville.

References

1. S. Houde-Walter, "Recent progress in gradient-index optics," in *Gradient-Index Optics and Miniature Optics*, D. C. Leiner and J. D. Rees, eds., Proc. SPIE **935,** 2–26 (1988).
2. W. Su, J. A. Gilbert, and C. Katsinis, "A photoelastic fiber optic strain gage," Exp. Mech. **35,** 71–76 (1995).
3. I. Abdulhalim and C. N. Pannel, "Photoelastically induced light modulation in gradient-index lenses," Opt. Lett. **18,** 1274–1276 (1993).
4. I. Kitano, K. Koizumi, and H. Matsumura, "A light-focusing fiber guide prepared by ion-exchange techniques," Jpn. J. Appl. Phys. **39,** 63–70 (1970).
5. P. O. Mclaughlin and D. T. Moore, "Models for the thermal expansion and temperature coefficient of the refractive index in gradient-index glass," J. Appl. Opt. **24,** 4342–4348 (1985).
6. P. O. Mclaughlin, and D. T. Moore, "Measurement of the differential thermal expansion and temperature dependence of refractive index in gradient-index glass," J. Appl. Opt. **24,** 4334–4341 (1985).
7. A. Brandenburg, "Stress in ion-exchanged glass waveguides," J. Lightwave Technol. **LT-4,** 1580–1590 (1986).
8. A. N. Miliou, R. Strivastava, and R. V. Ramaswamy, "Modeling of the index change in K^+Na^+ ion-exchanged glass," Appl. Opt. **30,** 674–680 (1991).
9. A. A. Appen, "Versuch zur klassifizierrung von komponenten nach ihrem einfluß auf die oberflächenspannung von silikatschmenlzen," Silikattechnik **5,** 113–124 (1954).
10. M. Shimizu, "Converging light transmitting body of high performance and process for production thereof," U.S. patent 4,462,663 (31 July 1984).
11. T. Miyazawa, K. Okada, T. Kubo, K. Nishizawa, I. Kitano, and K. Iga, "Aberration improvement of SELFOC lenses," Appl. Opt. **19,** 1113–1116 (1980).
12. S. T. Timoshenko and J. N. Goodier, *Theory of Elasticity* (McGraw-Hill, New York, 1970).
13. W. Su, "Photoelastic fiber-optic accelerometers," Ph.D. dissertation (University of Alabama in Huntsville, Huntsville, Alabama, 1995).
14. M. M. Frocht, *Photoelasticity* (Wiley, New York, 1948), Vol. II.
15. A. Kuske and G. Robertson, *Photoelastic Stress Analysis* (Wiley, New York, 1974).
16. R. A. Chipman, "Mechanics of polarization ray tracing," Opt. Eng. **34,** 1636–1645 (1995).
17. A. Sharma, D. V. Kumar, and A. K. Ghatak, "Tracing rays through gradient-index media: a new method," Appl. Opt. **21,** 984–987 (1982).
18. *SELFOC Product Guide* (Nippon Sheet Glass America, Inc., New York, 1992).
19. P. J. Sands, "Third-order aberrations of inhomogeneous lenses," J. Opt. Soc. Am. **60,** 1436–1443 (1970).